JOURNAL OF AIRCRAFT
Vol. 33, No. 3, May–June 1996

High-Lift Design Optimization Using Navier–Stokes Equations

S. Eyi* and K. D. Lee†
University of Illinois at Urbana–Champaign, Urbana, Illinois 61801
and
S. E. Rogers‡ and D. Kwak§
NASA Ames Research Center, Moffett Field, California 94035

This article presents a design optimization method for maximizing lift without increasing the drag of multielement airfoils at takeoff and landing configurations. It uses an incompressible Navier–Stokes flow solver (INS2D), a chimera overlaid grid system (PEGSUS), and a constrained numerical optimizer (DOT). Aerodynamic sensitivity derivatives are obtained using finite differencing. The method is first validated with single-element airfoil designs and then applied to three-element airfoil designs. Reliable design results are obtained at reasonable costs. Results demonstrate that numerical optimization can be an attractive design tool for the development of multielement high-lift systems.

Introduction

HIGH-LIFT aerodynamics is one of the pending items in the development of future transport aircraft. The current trend is toward a more efficient and simpler design to reduce weight and cost. The payload capacity of an aircraft can be increased by increasing the lift coefficient at a given angle of attack and the maximum lift coefficient, while reducing the drag coefficient. Reductions of wake vortices and aerodynamic noise are also in demand to improve airport capacity and transportation environment. An improvement in the high-lift system requires detailed understanding of flow physics to identify and eliminate causes of poor aerodynamic performances. High-lift systems involve both complex geometry and complex flow physics. They are usually composed of multiple elements such as leading-edge slats and multiple-slotted flaps, and include challenging flow physics such as turbulent flow separation, transition, confluent boundary layers, wakes, Reynolds number effects, three-dimensional effects, compressibility effects, etc. Recent progress in computational fluid dynamics (CFD) provides an unprecedented opportunity for understanding the complex flow physics and improving designs of high-lift systems.

Recently, there have been efforts to build high-lift analysis capabilities based on the Navier–Stokes technology. The prediction of the multielement flowfield has been remarkably improved by solving the Reynolds-averaged Navier–Stokes equations with proper turbulence models. Some approaches solved the incompressible Navier–Stokes equations,[1,2] and others used the compressible Navier–Stokes equations.[3,4] Different grid systems were adopted to accommodate the flowfield around multiple elements: chimera overlaid grids,[1–3] multizonal patched grids,[4] and unstructured grids.[5–7] Different turbulence models were incorporated: an algebraic model,[1,2,5] a one-equation model,[2,3,7] and a two-equation model.[2–4] Results imply that the choice of the turbulence model and grid system influences the quality of flow solution significantly. Although notable progress has been achieved, high-lift analysis technology still has room for improvement in both accuracy and efficiency. There are difficulties in accurately predicting the maximum lift condition and the flap boundary-layer separation. The transition model also effects flow solutions at high angles of attack.

A merit of CFD is its ability of providing detailed information on flowfields. Also, it has the unique design ability of finding a geometry producing desirable aerodynamic performance characteristics by solving an inverse problem.[8,9] However, it is often difficult either to formulate an inverse problem using high-level physics or to specify the target condition of a design. Therefore, optimization methods have been used to build design capabilities with various models of flow physics.[10–13] One advantage of optimization is that it uses an analysis capability to find improved designs. Multielement high-lift design optimizations were also attempted using the potential flow[14] and Euler physics,[15] coupled with boundary-layer analysis. A high-level flow model is preferred, because the reliability of a design result depends on the ability of accurately simulating the flowfield. The flow model used in a design process should be able to represent all of the significant flow physics involved.

In the present method, the flow is modeled with Navier–Stokes equations. One major concern of optimization-based design is the computational cost. However, its interest has been renewed because computational costs have been reduced significantly because of the advances in computer and numerical algorithm. The objective of the present study is to identify issues and bottlenecks associated with the design of multielement airfoils and to build an accurate multielement airfoil design tool using a reliable Navier–Stokes code. The design goal is to increase lift at a given angle of attack without increasing drag. In the following sections, the technology pieces used are first described and then results from design practices with single- and three-element airfoils are presented.

Flow Solver

Steady-state solutions of the incompressible Navier–Stokes equations are obtained using the INS2D computer code.[16] The

Presented as Paper 95-0477 at the AIAA 33rd Aerospace Sciences Meeting and Exhibit, Reno, NV, Jan. 9–12, 1995; received April 10, 1995; revision received Nov. 21, 1995; accepted for publication Dec. 27, 1995. Copyright © 1995 by the American Institute of Aeronautics and Astronautics, Inc. All rights reserved.

*Research Assistant, Department of Aeronautical and Astronautical Engineering. Student Member AIAA.

†Professor, Department of Aeronautical and Astronautical Engineering. Associate Fellow AIAA.

‡Aerospace Engineer, Fluid Dynamics Division. Member AIAA.

§Research Scientist, Fluid Dynamics Division. Associate Fellow AIAA.

code is based on the method of artificial compressibility in which a pseudo-time-derivative of pressure is added to the continuity equation. The convective part of the equations forms a hyperbolic system, which can be iterated in pseudotime until a steady-state solution is found. Since the convective terms of the resulting equations are hyperbolic, upwind differencing can be applied to these terms. The code uses a flux-difference splitting method. The upwind differencing leads to a more diagonally dominant system than does central differencing, and does not require an additional artificial dissipation. The system of equations is solved using a Gauss–Seidel-type line-relaxation scheme. The line-relaxation scheme is very useful for computing with multizonal grids because it makes it easy to iteratively pass the information on the change of dependent variables at each time step between the zone boundaries as the line-relaxation sweeping takes place. The result is a semi-implicit passing of boundary conditions between zones, which further enhances the code stability. The code has been proven robust and stable, which is the basic requirement to use in design optimization.

The turbulence model used in the present design optimization is the one-equation model developed by Baldwin and Barth.[17] It does not require an algebraic length scale and is derived from the simplified form of the standard two-equation k-ε model equations. The equation is solved using a line-relaxation procedure similar to that used for the mean-flow equations. The INS2D code is also equipped with the Baldwin–Lomax algebraic model and the k-ω two-equation turbulence model.[1,2] The Baldwin–Barth model gave significantly better results than the Baldwin–Lomax model. Although the two-equation model was proven to perform better in predicting the maximum lift in the multielement high-lift analysis,[2] the Baldwin–Barth model is used in the present study because of its robustness. The one-equation model takes less computer time and requires less grid points than the k-ω model.

Grid Topology

The chimera[18] overlaid grid system was used to discretize the flowfield around a multielement airfoil at takeoff and landing configurations. The chimera method of domain decomposition allows a system of relatively simple grids, adaptive to the geometry of each single component, to be combined into a composite grid system. The individual grids receive information from each other in the form of interpolated quantities. This communication occurs at two types of boundaries: at the outer boundary of a mesh that overlaps with the interior region of another mesh, and at an interior boundary surrounding a hole that is blanked out since its interior points lie inside of a solid body. The hole cutting and the formulation of interpolation stencils were performed with the PEGSUS software.

Figure 1 is an example of the chimera grid system for a three-element airfoil. It is the geometry used to investigate advanced multielement airfoils at high Reynolds numbers,[19] and used as a validation case for multielement airfoil analyses.[1,2] The composite mesh is composed of four grids: three C-grids around three elements of slat, main element, and flap, and an H-grid for the flap wake. Grid sizes are 121 × 31, 281 × 85, 121 × 41, and 21 × 37, respectively, with a total of 33,374 grid points. The chimera approach simplifies the grid generation task by providing a quality grid for each component. One disadvantage is the introduction of numerical boundary conditions in the interior of the flow domain. The present study uses the geometry and grid of Fig. 1 extensively in its three-element airfoil design optimization practices.

Numerical Optimization

The optimization of the present design study employs a commercial optimization package.[20] It finds feasible search directions and step sizes that minimize a specified objective function under a set of constraints. It searches for the values of design variables that minimize the Lagrangian formed with the objective function and constraints. The Kuhn–Tucker condition for optimality requires that the Lagrangian must have a vanishing gradient at the optimum values of design variables. The optimization process requires evaluation of sensitivity gradients of the objective and constraint functions with respect to design variables. In the present study, the sensitivity derivatives are evaluated using finite differencing.

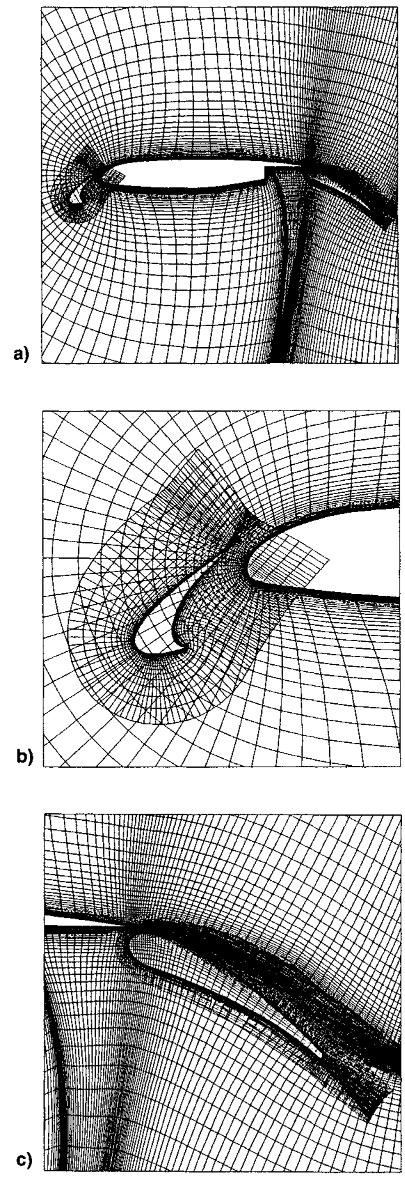

Fig. 1 Grids around a three-element airfoil: a) overall grid, b) slat near field, and c) flap near field.

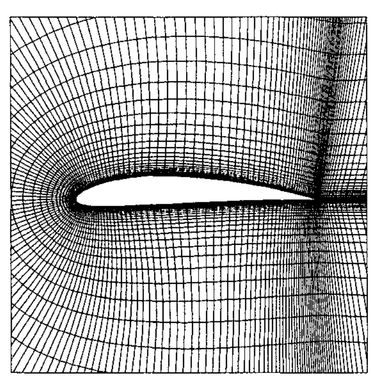

Fig. 2 Grid around the NACA 4412 airfoil.

The optimization process starts with an initial guess of the design variables. The design is then updated using an iterative procedure by finding the search direction (sensitivity gradient) and the step size to move into the direction. The optimum step size is found using a one-dimensional search via interpolation. The process is iterated until it converges to an optimum. The search direction must be usable and feasible. A usable direction is one that reduces the objective function, and a feasible direction is one that satisfies the constraints. When no constraints are active, the search direction is iteratively obtained using the Fletcher–Reeves conjugate direction method by imposing the orthogonality condition between search directions. An active constraint is one whose value becomes zero within some numerical tolerance. When some constraints are active or violated, a suboptimization process is used to find the search direction.

The optimization provides an efficient and systematic means of improving design. An improved design can always be guaranteed, even for strongly nonlinear problems with multiple

Table 1 Design optimization of the NACA 4412 airfoil at α = 13.87 deg

Parameter	Initial	Design	Change, %
C_l	1.659	1.740	4.88
C_d	0.0294	0.0293	−0.34
Area	0.0813	0.0813	0.00

Note: 80 function calls, 1794 flow iterations, 8.1 min.

Table 2 Design optimization of the NACA 4412 airfoil at α = 16.0 deg

Parameter	Initial	Design	Change, %
C_l	1.701	1.924	13.10
C_d	0.0452	0.0438	−4.20
Area	0.0813	0.0848	4.27

Note: 139 function calls, 8330 flow iterations, 37.4 min.

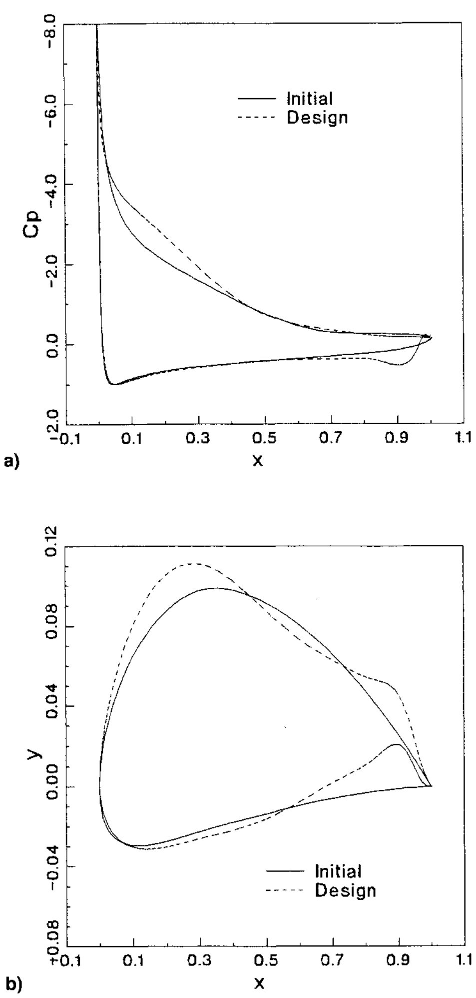

Fig. 3 Design optimization of the NACA 4412 airfoil at α = 16.0 deg: a) surface pressure and b) airfoil geometry.

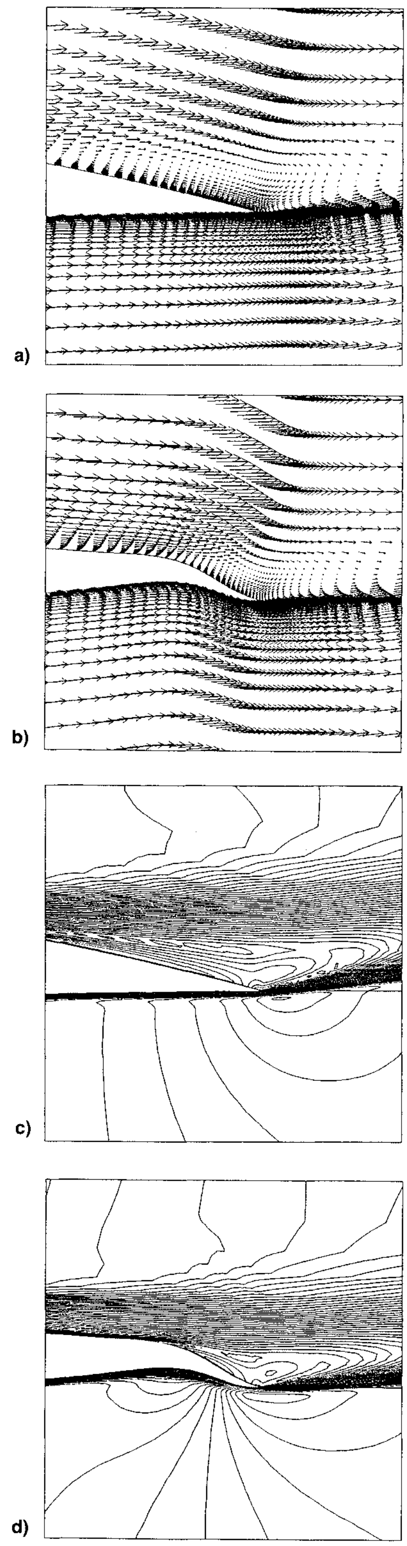

Fig. 4 Design optimization of the NACA 4412 airfoil at α = 16.0 deg: a) velocity vectors of NACA 4412, b) velocity vectors of designed airfoil, c) velocity contours of NACA 4412, and d) velocity contours of designed airfoil.

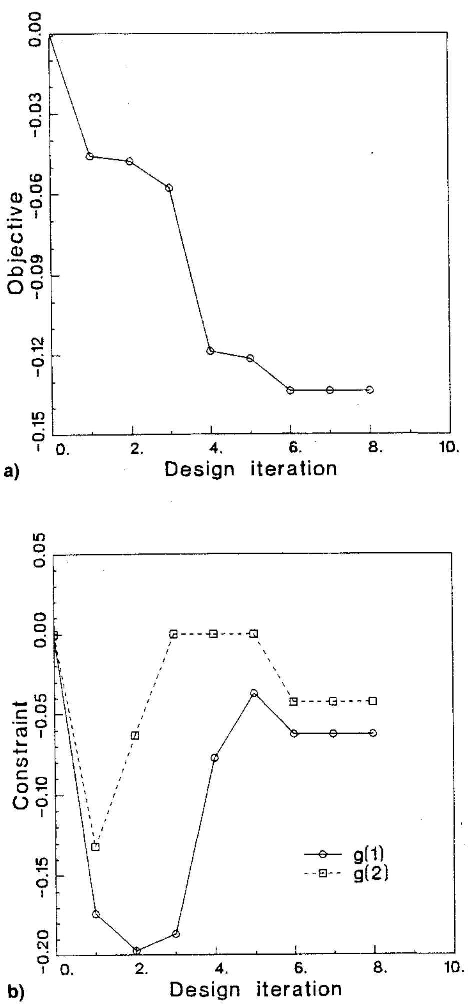

Fig. 5 Design optimization of the NACA 4412 airfoil at α = 16.0 deg: a) convergence of objective function and b) convergence of constraints.

constraints and design variables. The previous studies by the authors indicate that the efficiency and cost of a design depends on the number of design variables, the number of constraints, and the tolerance level of side constraints, because those dictate the number of function calls for flow analysis.

Demonstrations

The goal of the present design optimization was to increase lift and decrease drag at a given angle of attack. Side constraints were also imposed on design variables to accommodate the geometry limitations of high-lift systems. The high-lift design optimization was first performed for single-element airfoil designs to identify and investigate issues in Navier–Stokes design, and later extended to multielement high-lift configurations to evaluate the feasibility of using optimization for the development of high-lift systems.

Optimization of Single-Element Airfoil

Two designs were performed with the NACA 4412 airfoil at angles of attack of 13.87 and 16 deg. The former is the maximum-lift condition of the airfoil in experiment and the latter is a poststall condition. The grid is shown in Fig. 2. The grid size is 241 × 61. The Reynolds number was set to 1.5 × 10^6. The airfoil geometry was modified by adding smooth perturbations in both upper and lower surfaces of the airfoil. The geometry perturbation was defined as a linear combination of base functions. Fourteen Hicks–Henne[13] functions were used; seven each in upper and lower surfaces. Besides the constraint on drag, another constraint was imposed to avoid a reduction in the airfoil cross-sectional area. The optimization process was started with the analysis solution of the baseline airfoil. The iteration was terminated when it converged to a specified tolerance or reached the maximum number of iterations specified. Each function call corresponds to one analysis run with INS2D. Function calls within the optimization process took much less iterations than the regular analysis because they were initialized with the most recent available solutions.

Tables 1 and 2 compare aerodynamic characteristics between the initial and designed airfoils at angles of attack of 13.87 and 16 deg, respectively. The design cycle was terminated when there were no changes in the objective function and constraints in two subsequent cycles. The α = 13.87-deg design took 80 function calls, but only 11 times the iterations required for the regular analysis. In comparison, the α = 16.0-deg design required 139 function calls that are about 33 times the iterations for the analysis. In both cases, the design objective of increasing lift was achieved and constraints were satisfied. Figure 3 compares surface pressures and airfoil geometries between the initial and designed airfoils at α = 16.0 deg. An interesting observation is that in the α = 16.0-deg design the optimization made a flap out of the aft portion of the airfoil, resulting in a large increase of lift. Figure 4 compares velocity vectors and velocity magnitude contours between the original and designed airfoils, showing a smaller separated flow region with the designed airfoil.

A parametric study was performed to evaluate the performance, dependency, consistency, and cost of the present design optimization method. The performance of the optimization process is shown in Fig. 5. It was found to be strongly case dependent. It may be attributed to the strongly nonlinear flow-

Table 3 Design optimization of a three-element airfoil at α = 8.10 deg

Parameter	Initial	Design	Change, %
	Slat setting[a]		
C_l	2.490	2.537	1.88
C_d	0.1035	0.0950	−8.24
	Flap setting[b]		
C_l	2.490	2.528	1.52
C_d	0.1035	0.1035	−0.05
	Slat and flap setting[c]		
C_l	2.490	2.561	2.84
C_d	0.1035	0.0941	−9.10

[a]15 function calls, 2047 flow iterations, 27.1 min.
[b]14 function calls, 1993 flow iterations, 26.2 min.
[c]21 function calls, 2923 flow iterations, 38.4 min.

Table 4 Design optimization of a three-element airfoil at α = 16.21 deg

Parameter	Initial	Design	Change, %
	Slat setting[a]		
C_l	3.379	3.489	3.26
C_d	0.1094	0.1032	−5.65
	Flap setting[b]		
C_l	3.379	3.403	0.71
C_d	0.1094	0.1086	−0.75
	Slat and flap setting[c]		
C_l	3.379	3.515	4.02
C_d	0.1094	0.0961	−12.22

[a]29 function calls, 3428 flow iterations, 45.2 min.
[b]20 function calls, 2917 flow iterations, 38.3 min.
[c]39 function calls, 4327 flow iterations, 56.9 min.

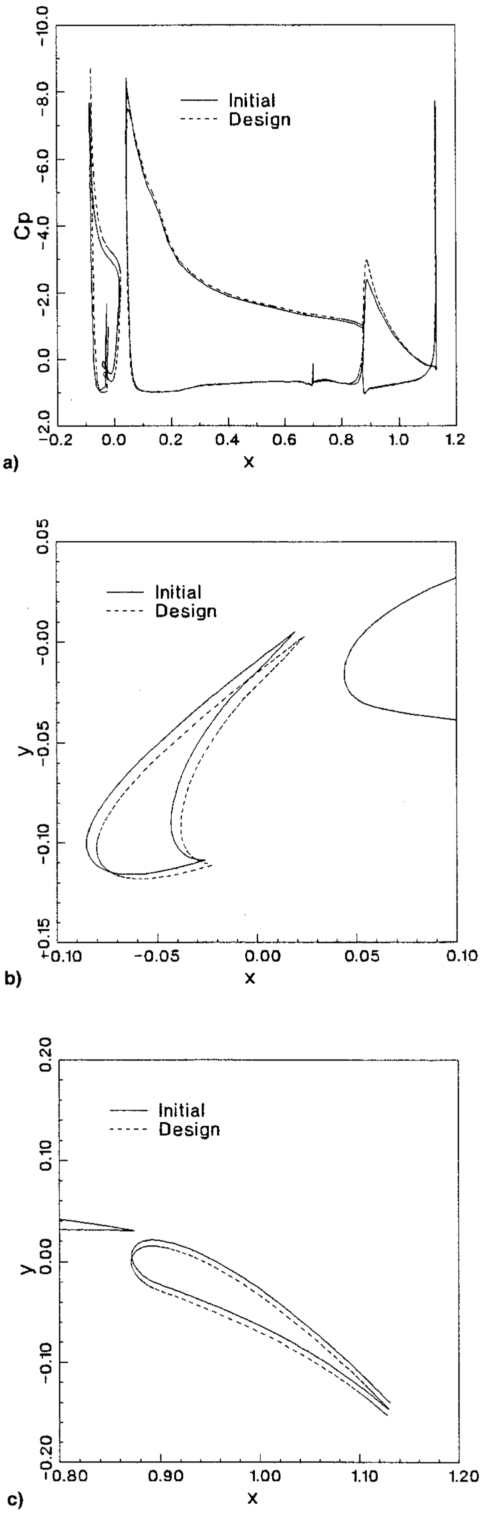

Fig. 6 Optimization of slat and flap setting for a three-element airfoil at $\alpha = 16.21$ deg: a) surface pressure, b) slat setting, and c) flap setting.

field with complex flow physics. The optimization efficiency is sensitive to design parameters such as the flow condition, the number of design variables, the number of constraints, the step size in finite difference sensitivity evaluation, the tolerance in solution iteration, etc. However, it never failed to find a better design.

Optimization of Multielement Airfoil

A three-element airfoil in a landing configuration given in Ref. 19 was used to examine the efficiency of the present design optimization process. The slat and flap were both deflected 30 deg, and the Reynolds number was set to 9×10^6. To reduce the computational cost, the grids in Fig. 1 were used in the present study, although better flow predictions were obtained with enhanced grid resolution at the slat trailing-edge region.[2] The high-lift optimization was performed at two angles of attack of 8.10 and 16.21 deg. As a first step for the multielement airfoil design, the design optimization was performed with a small number of design variables. The design variables used were relative positions between multiple elements: gap, rotation, and overhang. The geometry of each element was kept unchanged in the present study. The purpose of this practice was to duplicate the recent similar optimization efforts conducted experimentally.[19,21] Three cases are presented: slat setting, flap setting, and both slat and flap setting.

Tables 3 and 4 show the optimum slat setting, flap setting, and slat/flap setting at angles of attack of 8.10 and 16.21 deg, respectively. Only cases with gap and rotation as design variables are reported because overhang did not contribute to any remarkable gains in the design objective in all three cases. Results demonstrate that substantial gains of increasing lift and reducing drag were obtained at relatively low costs in all cases. The number of flow iterations shown includes that for the analysis run. On the grids shown in Fig. 1, the flow analysis requires 223 iterations for $\alpha = 8.10$ deg and 732 for $\alpha = 16.21$ deg to obtain converged solutions. In all calculations, flow iterations were terminated when the residual was reduced by four orders of magnitude from its freestream value. Figure 6 shows the results of a multielement airfoil design for slat and

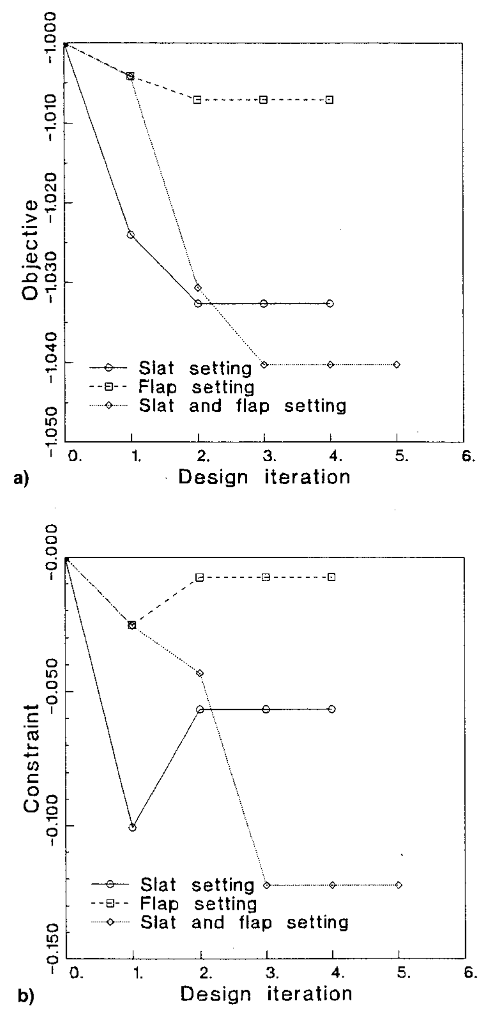

Fig. 7 Optimization of slat and flap setting for a three-element airfoil at $\alpha = 16.21$ deg: a) convergence of objective function and b) convergence of constraint.

flap setting at $\alpha = 16.21$ deg, and Fig. 7 exhibits the convergence of the optimization process. Grids were regenerated before each function call of flow analysis, sensitivity derivative evaluation, or optimum step-size search. With the present grids, one flow iteration costs 0.76 CPU seconds on Cray C-90, and the cost of one complete grid regeneration is equivalent to that of four flow iterations.

Unlike single-element airfoil optimization, multielement airfoil design optimization requires strict side constraints on design variables to account for the limitations imposed on the geometry and relative position of airfoil elements. Even with the present limited experience, it is found that the optimization process of multielement airfoil design is often dictated by the side constraints. Side constraints are imposed to accommodate the geometry at the cruise condition and the control mechanism of the high-lift system. Side constraints are also needed because of the limitations on the flow solver and the grid generator used in the optimization. The whole optimization process can easily diverge if a design variable changes beyond its limits. The optimization process often suffered with the issue associated with local minimum, especially in multielement design optimization. That is, instead of reaching the global minimum point, the optimization becomes stagnant at a local minimum, terminating the design cycle with a smaller gain in design objective. This explains why different designs resulted when different design parameters were used at the same design condition.

Conclusions

A design optimization method that improves high-lift characteristics of multielement airfoils was presented. It uses an incompressible Navier–Stokes code with the one-equation Baldwin–Barth turbulence model, a chimera overlaid grid system, and a numerical optimizer using finite difference sensitivity evaluations. The presented design practices demonstrate that Navier–Stokes designs are feasible for the high-lift system development in the current computing environment. Design efficiency can be significantly enhanced through a careful choice of design variables. A successful optimization process requires a robust Navier–Stokes code to improve the confidence level of a design result. The present study implies that one major issue in Navier–Stokes design is the handling of local minimum, as well as the reduction of design cost. Future plans with the present multielement airfoil design optimization approach include geometry modification, maximum-lift improvement, and multipoint design.

Acknowledgments

This research was partially funded by NASA Ames Research Center through Research Grant NCA2-833. The computing time for this study was provided by the Numerical Aerodynamic Simulation (NAS) System at NASA Ames Research Center.

References

[1]Rogers, S. E., Wiltberger, N. L., and Kwak, D., "Efficient Simulation of Incompressible Viscous Flow over Single and Multi-Element Airfoils," AIAA Paper 92-0405, Jan. 1992.

[2]Rogers, S. E., "Progress in High-Lift Aerodynamic Calculations," AIAA Paper 93-0194, Jan. 1993.

[3]Mani, M., and Bush, R. H., "Overlapping Grid Method for High-Lift and Store Carriage Applications," *Proceedings of AIAA 11th Applied Aerodynamics Conference* (Monterey, CA), AIAA, Washington, DC, 1993.

[4]Egami, K., Shima, E., Nakamura, S., and Amano, K., "Two-Dimensional Navier-Stokes Analysis of High-Lift Multi-Element Airfoils Using the q-ω Turbulence Model," AIAA Paper 93-0679, Jan. 1993.

[5]Mavriplis, D. J., "Algebraic Turbulence Modeling for Unstructured and Adaptive Meshes," *AIAA Journal*, Vol. 29, No. 12, 1991, pp. 2086–2093.

[6]Mavriplis, D. J., and Martinelli, L., "Multigrid Solution of Compressible Turbulence Flow on Unstructured Meshes Using a Two-Equation Model," AIAA Paper 91-0237, Jan. 1991.

[7]Anderson, W. K., and Bonhaus, D. L., "Navier-Stokes Computations and Experimental Comparisons for Multielement Airfoil Configurations," AIAA Paper 93-0645, Jan. 1993.

[8]Volpe, G., and Melnik, R. E., "The Design of Transonic Airfoils by a Well-Posed Inverse Method," International Conf. on Inverse Design Concepts in Engineering Sciences, Austin, TX, Oct. 1984.

[9]Giles, M. B., and Drela, M., "Two-Dimensional Transonic Aerodynamic Design Method," *AIAA Journal*, Vol. 25, No. 9, 1987, pp. 1199–1205.

[10]Haney, H. P., Johnson, R. R., and Hicks, R. M., "Computational Optimization and Wind Tunnel Test of Transonic Wing Designs," *Journal of Aircraft*, Vol. 17, No. 7, 1980, pp. 457–463.

[11]Lee, K. D., and Eyi, S., "Transonic Airfoil Design by Constrained Optimization," *Proceedings of the AIAA 9th Applied Aerodynamics Conference* (Baltimore, MD), AIAA, Washington, DC, 1991, pp. 677–687.

[12]Malone, J. B., Narramore, J. C., and Sankar, L. N., "Airfoil Design Method Using the Navier-Stokes Equations," *Journal of Aircraft*, Vol. 28, No. 3, 1991, pp. 216–224.

[13]Eyi, S., Hager, J. O., and Lee, K. D., "Airfoil Design Using the Navier-Stokes Equations," *Journal of Optimization Theory and Applications*, Vol. 83, No. 3, 1994, pp. 447–461.

[14]Olson, L. E., "Optimization of Multielement Airfoils for Maximum Lift," *Advanced Technology Airfoil Research*, Vol. I, NASA CP 2045, 1979, pp. 237–253.

[15]Drela, M., "Design and Optimization Method for Multi-Element Airfoils," AIAA Paper 93-0969, Feb. 1993.

[16]Rogers, S. E., and Kwak, D., "An Upwind Differencing Scheme for the Steady-State Incompressible Navier-Stokes Equations," *Journal of Applied Numerical Mathematics*, Vol. 8, No. 1, 1991, pp. 43–64.

[17]Baldwin, B., and Barth, T., "A One-Equation Turbulence Transport Model for High-Reynolds Number Wall-Bounded Flows," AIAA Paper 91-0610, Jan. 1991.

[18]Benek, J. A., Buning, P. G., and Steger, J. L., "A 3-D Chimera Grid Embedding Technique," *AIAA 7th Computational Fluid Dynamics Conference*, AIAA, New York, 1985, pp. 322–331.

[19]Valarezo, W. O., Dominik, C. J., McGhee, R. J., Goodman, W. L., and Paschal, K. B., "Multi-Element Airfoil Optimization for Maximum Lift at High Reynolds Numbers," *Proceedings of the AIAA 9th Applied Aerodynamics Conference*, AIAA, Washington, DC, 1991, pp. 969–976.

[20]Vanderplaats, G. N., and Hansen, S. R., "Dot Users Manual," VMA Engineering, Goleta, CA, 1989.

[21]Moir, I. R. M., "An Experimental Investigation of the Optimum Slat Setting on a Combat Aircraft Model," *High-Lift System Aerodynamics*, CP-515, AGARD, Sept. 1993, pp. 17.1–17.16.